An analysis of the birdcage resonators using magnetic field probes, for validation of optimal aspect ratio

K. Jurik[1] and P. Drexler[1]

[1]Brno University of Technology, FEEC, DTEEE, Czech Republic

E-mail: karel.jurik@vut.cz, drexler@vut.cz

Abstract—Two probes were created in order to analyse the magnetic field of the birdcage resonators with different heights and aspect ratios. The first probe has a larger pickup loop at its end and was shielded to reduce the electric field coupling. The second probe with a smaller loop was not shielded at its end. The relative values of magnetic field intensity obtained using the two probes were similar, however, the first probe has better sensitivity. Both measurements confirm that there exists an optimal height and, therefore, an aspect ratio, of the resonators with respect to the generated magnetic field intensity.

Keywords—birdcage resonator, magnetic field probe, pick-up loop, current probe

1. INTRODUCTION

Birdcage resonators (sometimes referred to as birdcage coils) are usually used as the transmitting or receiving coils in magnetic resonance imaging (MRI) instruments. The resonators consist of even number of legs and two endrings at their ends. There are also capacitors, placed in the legs or in the endrings, which together with the inductance of the conductors creates the resonance [1]. If the capacitors are placed in the endrings, the resonator is high-pass type, if the capacitors are in the legs a low-pass type is created. There is also a combination of the two foregoing structures: a band-pass resonator (the three types are visualised in Figure 1). Each resonator has N/2 resonant modes, where N is the number of legs. One of these modes (for high-pass the mode located at the highest frequency, for low-pass at the lowest frequency) possesses the cosine distribution of currents around its circumference, therefore creating a homogeneous magnetic field inside its volume. For high-pass type, two more resonant modes can be found (anti-rotational and co-rotational) which are associated with the resonance of the endrings themselves [2]. After the invention of the birdcage resonators, the description of their resonance modes relied mainly on analytical solution and lumped-element analysis [3]. With the increasing frequency of operation, the parasitic behaviour (such as radiation) became important, and the purely lumped-element approach was not accurate anymore. Then, the methods of numerical analysis started to be used more frequently for birdcage resonator diagnostics [4].

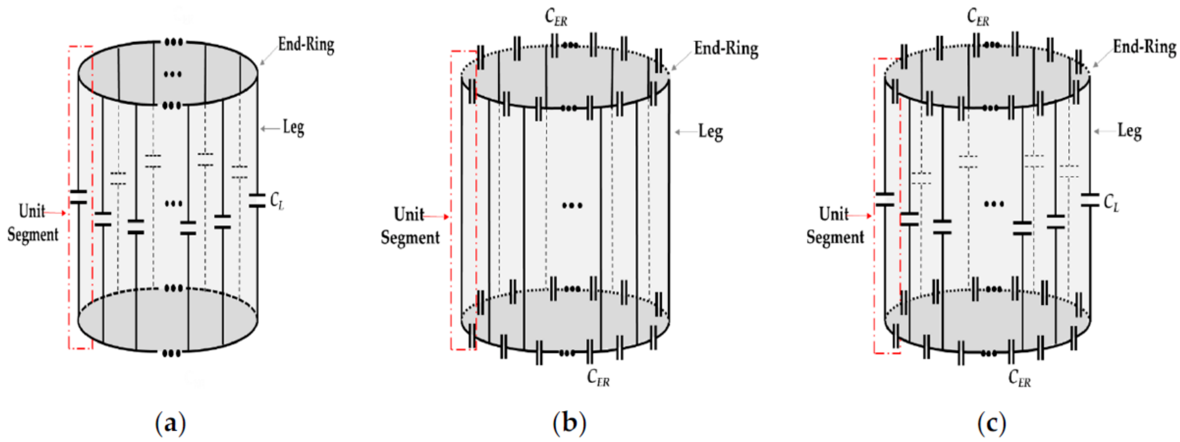

Figure 1: Different types of birdcage resonators - a) low-pass, b) high-pass, c) band-pass. Adapted from [5].

2. NUMERICAL ANALYSIS

Five high-pass birdcage resonators are analysed within this paper. The resonators differ in the capacity of inserted capacitors (Johanson Technology: SMD 0805, High-Q, 250 V), which ranges from 4.7 pF to 12 pF. The parameters of the examined resonators were simulated using Ansys HFSS. The diameter was fixed to 40 mm for all resonators and their height was adjusted to meet the frequency of 433 MHz of the fundamental resonance mode. The results of the analysis were already published and are described in detail in [6]. From the perspective of this paper, the most important is the information about the magnetic field in the middle of the resonator and the calculated resonator's height (Figure 2). The analysis results show clearly, that with increasing inserted capacity, therefore, decreasing height of the resonators, the magnetic field intensity in their centre is increasing.

However, the magnetic field is homogeneous only in the central part of the resonator. Closer to the endrings, the intensity of the field is decreasing. Therefore, the resonators with low aspect ratio (the resonators with the inserted capacity of 10 and 12 pF in this paper) are not suitable for MRI, since the volume of homogeneous magnetic field is restricted. For alternative application of the birdcage resonators (such as plasma processing [7]) these resonators might still be useful. The comparison of two examples with different volumes of homogeneous magnetic field is shown in Figure 3.

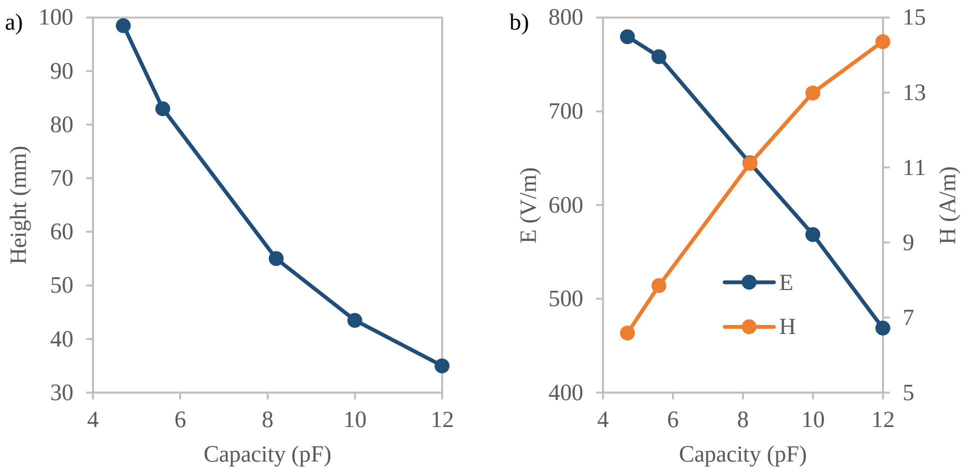

Figure 2: a) Height, b) Electric and magnetic field intensity in dependence on the inserted capacity. Adapted from [6].

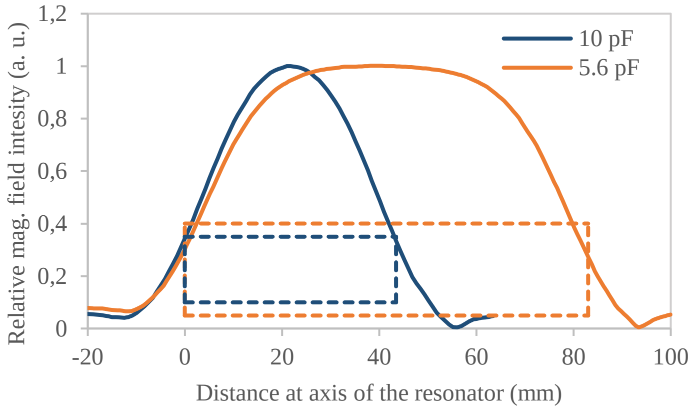

Figure 3: An example of the magnetic field distribution for the resonators with different heights (with 5.6 and 10 pF capacitors. The resonators are represented with dashed lines. Adapted from [6].

3. EXPERIMENTAL SETUP

Two magnetic probes were created of semi-rigid coaxial cable (RG-405CU, QAXIAL). The first probe was created by bending a whole coaxial cable with respect to its minimum bending diameter, and the centre conductor was then soldered to the outer shield to create a closed loop with a diameter approximately of 10 mm. The outer conductor shields the loop, which helps to reduce the response of the probe to the electric field created by the resonator. The second probe was fabricated with respect to higher spatial resolution. The outer shield was removed, and the loop was created by the central conductor only. The loop has diameter of approx. 3.5 mm. Both probes were completed with an SMA connector (Figure 4). The previously prepared birdcage resonators [6] were matched to 50 Ω by a variable capacitor in series with the resonator, and together with the probes were placed to a 3D printed fixture, which ensures the proper centring of the probe inside the birdcage resonator (Figure 5).

The matched birdcage resonators and the probe were connected to vector network analyser (VNA) Rohde & Schwarz ZVL (0–6 GHz), and the magnetic field intensity was measured as the S_{21} parameter between the ports of the VNA. The S_{21} parameter was measured after fine-tuning of the adjustable capacitor (insertion of the probe caused a slight change in the impedance) and the maximal value was recorded. The measurement was done in the middle of the height of the resonator, and the plane of the probe loop was aligned perpendicular to the feeding point.

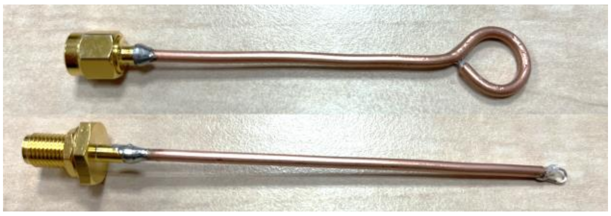

Figure 4: Magnetic field probes

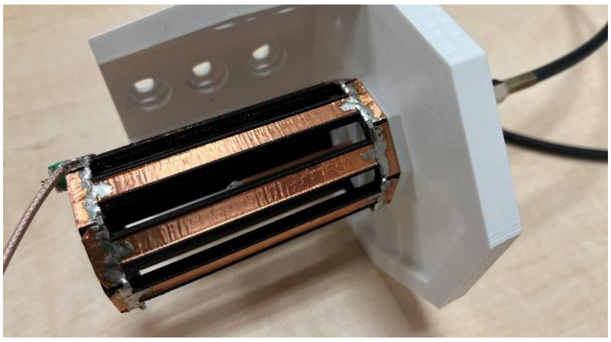

Figure 5: Measurement setup (the probe is located in the centre of the resonator)

4. RESULTS AND DISCUSSION

Figure 6 shows the dependence of the measured S_{21} parameters on the height of the resonators (see Figure 2 a)) for comparison with the capacity of the inserted capacitors. Both measurements show that the resonator with 8.2 pF inserted capacity possesses the most intense magnetic field in the middle of its height. The results are in accordance with the assumptions from the analytical calculation, which states that "the magnetic field amplitude at the centre is maximum when the length to diameter ratio is equal to √2" [2]. For 40 mm of diameter, the optimal height is approx. 56.6 mm, which corresponds to the maximum in Figure below, which is located at 55 mm.

Besides the agreement of the analytical solution and the measured values, a discrepancy between the results of the simulation (Figure 2 b)) and measurement was found. According to the simulation, the magnetic field intensity should decrease with the increasing height of the resonators across the whole range of evaluated heights. However, the results of the simulation show only the maximum of magnetic field intensity in the centre of the resonator, while the probes are measuring the proximate surroundings as well. To diagnose this discrepancy, the results of the simulation were interpreted in a different way. The magnetic field intensity was cumulated (a sum was calculated over 201 points) in the range -0.5 mm to 0.5 mm around the centre of the resonator. The calculated values are compared to the S_{21} parameters measured with the smaller probe in Figure 7. There is still a discrepancy between the simulation and measurement, however the trends agree. The discrepancy is probably caused by non-ideal behaviour of the fabricated prototypes.

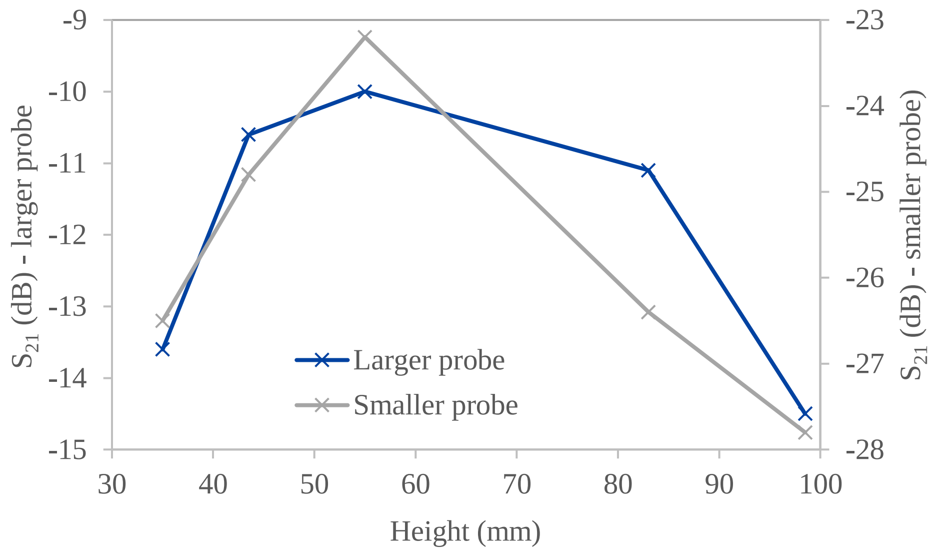

Figure 6: Measured S_{21} parameters for two magnetic field probes

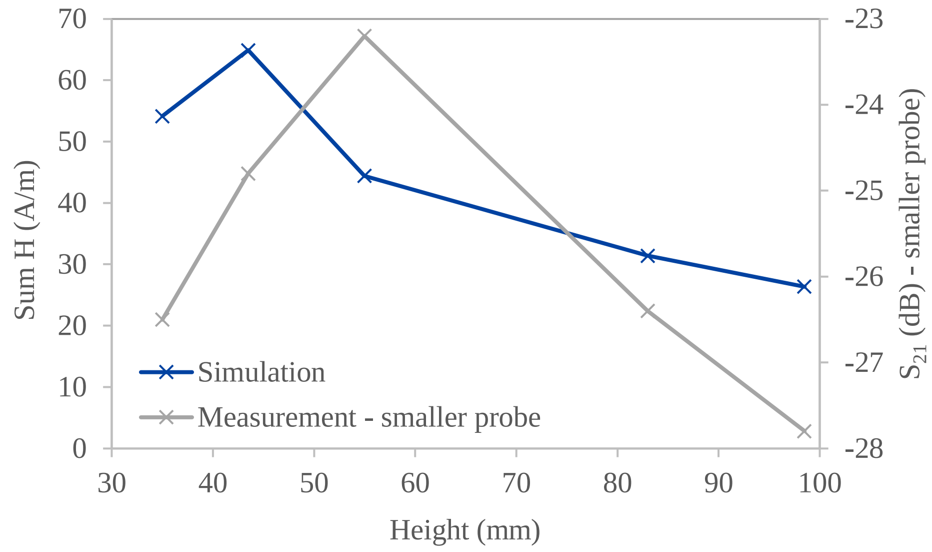

Figure 7: Comparison of simulation and measurement using the smaller probe

5. CONCLUSION

The measurement with both probes confirms that there exists an optimal aspect ratio of the birdcage resonators, with respect to the created magnetic field intensity. The best results were achieved for the birdcage with a height of 55 mm. The probe with the smaller loop at its end exhibits lower sensitivity to the magnetic field, however, the measured intensity is steeper decreasing towards the non-optimal aspect ratios.

ACKNOWLEDGMENT

This work has been supported by grant FEKT-K-22-7732 realised within the project Quality Internal Grants of BUT (KInG BUT), Reg. No. CZ.02.2.69 / 0.0 / 0.0 / 19_073 / 0016948, which is financed from the OP RDE.

REFERENCES

[1] C. Hayes, W. Edelstein, J. Schenck, O. Mueller and M. Eash, "An efficient, highly homogeneous radiofrequency coil for whole-body NMR imaging at 1.5 T", Journal of Magnetic Resonance (1969), vol. 63, no. 3, pp. 622-628, 1985.

[2] J. Mispelter, M. Lupu, and A. Briguet, “NMR Probeheads for Biophysical and Biomedical Experiments”

[3] R. Pascone, et al., "Generalized electrical analysis of low-pass and high-pass birdcage resonators", Magnetic Resonance Imaging, vol. 9, no. 3, pp. 395-408, 1991.

[4] N. Gurler and Y. Z. Ider, “Numerical methods and software tools for simulation, design, and resonant mode analysis of radio frequency birdcage coils used in MRI”, Concepts in Magnetic Resonance Part B: Magnetic Resonance Engineering, vol. 45, no. 1, pp. 13-32, 2015.

[5] S. F. Ahmad, Y. C. Kim, I. C. Choi, and H. D. Kim, “Recent Progress in Birdcage RF Coil Technology for MRI System”, Diagnostics, vol. 10, no. 12, 2020.

[6] K. Jurik, P. Drexler, D. Nespor, and L. Havlicek, “Parametric Optimization of a Birdcage Resonator for Low-pressure Plasma Excitation”, pp. 455-461, Nov. 2021.

[7] P. Guittienne, R. Jacquier, B. Pouradier Duteil, A. A. Howling, R. Agnello, and I. Furno, “Helicon wave plasma generated by a resonant birdcage antenna: magnetic field measurements and analysis in the RAID linear device”, Plasma Sources Science and Technology, vol. 30, no. 7, Jul. 2021.